

Adhesion of *Pseudomonas fluorescens* biofilms to glass, stainless steel and cellulose

W. R. Z. Wan Dagang · J. Bowen ·
J. O’Keeffe · P. T. Robbins · Z. Zhang

Received: 30 August 2015 / Accepted: 21 January 2016 / Published online: 18 February 2016
© Springer Science+Business Media Dordrecht 2016

Abstract

Objectives The adhesion of colloidal probes of stainless steel, glass and cellulose to *Pseudomonas fluorescens* biofilms was examined using atomic force microscopy (AFM) to allow comparisons between surfaces to which biofilms might adhere.

Results Biofilm was grown on a stainless steel substrate and covered most of the surface after 96 h. AFM approach and retraction curves were obtained when the biofilm was immersed in a tryptone/soy medium. On approach, all the colloidal probes experienced a long non-contact phase more than 100 nm in

length, possibly due to the steric repulsion by extracellular polymers from the biofilm and hydrophobic effects. Retraction data showed that the adhesion varied from position to position on the biofilm. The mean value of adhesion of glass to the biofilm (48 ± 7 nN) was the greatest, followed by stainless steel (30 ± 7 nN) and cellulose (7.8 ± 0.4 nN).

Conclusion The method allows understanding of adhesion between the three materials and biofilm, and development of a better strategy to remove the biofilm from these surfaces relevant to different industrial applications.

Keywords Adhesion · Atomic force microscopy · Biofilm · Colloidal probe · *Pseudomonas fluorescens* · Repulsion

Introduction

Microorganisms can develop biofilms on many surfaces. Characterising biofilm adhesion is challenging, particularly during the early stages of formation when the thickness is small. An alternative is measuring adhesive forces directly using atomic force microscopy (AFM).

AFM can be used to measure forces in the nanoNewton to picoNewton range (Dorobantu et al. 2012) and is therefore appropriate for characterising bacterial adhesion. However, rather than attach a

-
- A1 W. R. Z. Wan Dagang
A2 Faculty of Biosciences and Medical Engineering,
A3 Universiti Teknologi Malaysia, UTM Skudai,
A4 81310 Johor Bahru, Malaysia
A5 e-mail: rosmiza@utm.my
- A6 J. Bowen
A7 Department of Engineering and Innovation, The Open
A8 University, Walton Hall, Milton Keynes MK7 6AA, UK
A9 e-mail: james.bowen@open.ac.uk
- A10 J. O’Keeffe
A11 Unilever R&D, Port Sunlight, Bebington, Wirral, UK
A12 e-mail: o’keeffe@unilever.com
- A13 P. T. Robbins · Z. Zhang (✉)
A14 School of Chemical Engineering, University of
A15 Birmingham, Birmingham B15 2TT, UK
A16 e-mail: z.zhang@bham.ac.uk
- A17 P. T. Robbins
A18 e-mail: p.t.robbins@bham.ac.uk

single cell to a tipless cantilever (Kang and Elimelech 2009) and investigate its adhesion to different surfaces, the approach here followed that of Puricelli et al. (2015) in sourcing colloid probes of stainless steel, glass and cellulose, attaching these to AFM cantilevers, and measuring their adhesion to biofilms of *Pseudomonas fluorescens*, chosen as a model organism. These materials have wide applications in industry. It was presumed their adhesion to the surface of a biofilm would also represent adhesion of a biofilm to them.

At neutral pH, bacteria and most inert surfaces are negatively charged whilst the size of bacteria in biofilms is similar to that of colloidal particles. This suggests that classical Deyaguin–Landau–Verwey–Overbeek (DLVO) theory might be used to describe bacterial adhesion to surfaces. However, there can also be hydrophobic interactions in bacterial adhesion and self-agglutination (Liu et al. 2004; Shephard et al. 2010). van Oss et al. (1988) extended DLVO theory to include such hydrophobic interactions. It is also possible that steric repulsion due to extracellular polysaccharides (EPS) may affect adhesion (Li and Logan 2004). AFM data were interpreted in light of these considerations.

Materials and methods

Single stainless steel (READE), glass (Polysciences Inc) and cellulose (Sigma Aldrich) colloidal microparticle probes were attached to a tipless AFM cantilever (NCL-20, Windsor Scientific Ltd.) with epoxy resin (Fig. 1).

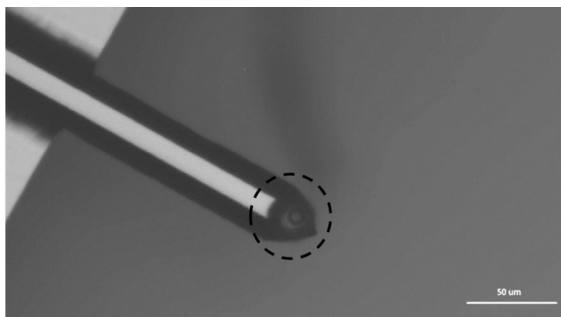


Fig. 1 Microscopic image of a glass colloidal probe of approximate diameter 20 μm immobilized at the apex of a tipless atomic force microscope cantilever (dashed-line circle). Scale bar = 50 μm

Pseudomonas fluorescens NCIMB 9046 biofilms were prepared and their morphology characterised using confocal laser scanning microscopy, as described in Fig. 2.

The biofilm was covered with tryptone/soy medium during force measurements. A NanoWizard II atomic force microscope with CellHesion module (JPK Instruments) was used to generate approach and retraction force-distance curves for each probe type. For each probe two biofilms were tested, each at 6 different positions.

Results

Figure 2 shows that most of the substrate surface was covered by biofilm about 33 μm thick. The volumes of EPS, live and dead cells were 62, 55 and 28 μm^3 respectively. There appeared to be a substantial polymer (EPS) layer at the surface of the biofilm.

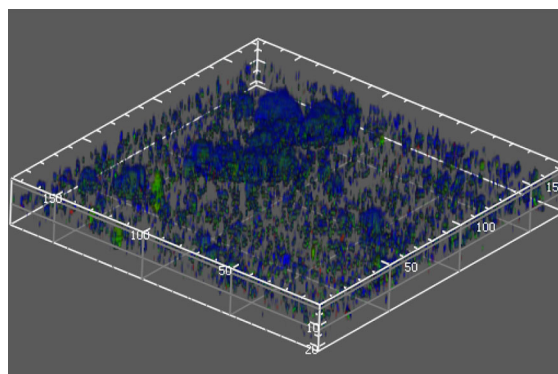


Fig. 2 Three-dimensional confocal laser microscopic image of a 174.6 μm square, 96 h old, *P. fluorescens* biofilm on a stainless steel substrate. The substrates were prepared by soaking in 1 % (w/v) Virkon solution overnight, in acetone for 30 min, and in 1 M sodium hydroxide solution for 1 h, with intermediate and final rinses with distilled water, followed by drying at 60 $^{\circ}\text{C}$ for 1–2 h. Clean dry substrates were autoclaved at 121 $^{\circ}\text{C}$ for 15 min in tryptone soy medium containing 0.25 % (w/v) glucose, which was then inoculated with approximately 10^6 cells ml^{-1} of *P. fluorescens* from an overnight shake flask culture. After 96 h at 25 $^{\circ}\text{C}$, the biofilm on the substrate was rinsed twice with phosphate buffer solution. It was then stained with a BacLight bacterial viability kit and Calcofluor White M2R (Sigma-Aldrich) and then imaged under oil immersion using TSC SPE confocal laser scanning microscopy (Leica Microsystems). Images were processed using *daime* software (Daims et al. 2006) to identify live cells (green), dead cells (red) and extracellular polysaccharides (blue). A series of images was taken in the vertical direction at 2 μm intervals

Example approach curves for all probe types are shown in Fig. 3. Considering the approach curve for stainless steel as an example, no interaction was observed when the separation distance was over 150 nm. There was then a non-linear interaction from 150 to 0 nm (contact with the biofilm surface), by which time the cantilever was deflected up to 16 nm due to a repulsive force. Once contact was made, further increase in repulsion was observed from distance of 0 to -29 nm. The biofilm was then indented by the probe in the so-called constant compliance region where the deflection and distance vary linearly. The glass probe showed similar behaviour but there appeared to be very long range interactions for the cellulose probe.

Upon approaching the biofilm, the cellulose probe experienced a strong repulsive force with a mean of total non-linear distance of 670 ± 90 nm as presented in Table 1. The repulsive interaction was weaker for stainless steel and glass (72 and 69 % decrease of total non-linear distance, respectively).

A typical retraction curve for a stainless steel colloidal probe is shown in Fig. 4. The slope in the constant compliance region was nearly constant as the cantilever was moved away from the cell. The probe was then pulled off the biofilm until the adhesive force was zero and there was no longer interaction between probe and biofilm. The maximum adhesive force was 8.1 nN in this case.

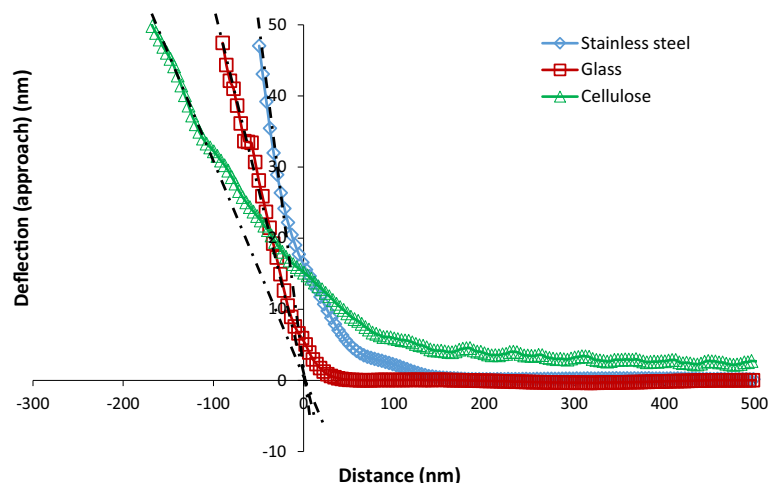


Fig. 3 Representative approach curves for stainless steel (*open diamond*), glass (*open square*) and cellulose (*open triangle*) colloidal probes to *P. fluorescens* biofilms. Adhesion measurements were performed in contact mode with an approach velocity of $20 \mu\text{m s}^{-1}$ and compressive load of 100 nN. The

All maximum adhesive forces are shown in Fig. 5. Although the adhesive forces varied from position to position on the biofilm, stainless steel and glass probes showed generally greater adhesion (30 ± 7 nN; range 6–68 nN and 48 ± 7 nN; range 9–94 nN respectively) than cellulose (7.8 ± 0.4 nN; range 5–13 nN). The general trend was greatest adhesion of *P. fluorescens* biofilm to glass, followed by stainless steel, and finally cellulose.

Discussion

Upon approaching the biofilm surfaces, all the probes experienced a non-contact phase over 100 nm long (Fig. 3). This is well beyond the likely range of electrostatic or van der Waals forces. It is probable that there may have been steric repulsion due to the existent polymer brushes of EPS on the biofilm surface (Jasevicius et al. 2015). The differences between the probes in the non-contact region might also be due to their hydrophobicity. Stainless steel is more hydrophobic than glass (Butt 1994) and cellulose (Karlsson and Gatenholm 1999). The hydrophilic nature of cellulose would result in its increased difficulty in approaching the biofilm, as suggested by the long non-contact region visible in Fig. 3. This supports suggestions that classical DLVO theory provides poor agreement with experimental

cantilever spring constant was calibrated according to the method described by Bowen et al. (2010), which is 40 N/m. Approach curves were analysed by extrapolating the linear constant compliance region to the horizontal axis, in order to define the zero position of the cantilever movement

Table 1 Mean position relative to the biofilm surface of non-contact interactions, the mean length of the contact phase and the total non-linear region from analysis of approach curves

Probe material	Non-contact interactions (nm)	Contact phase (nm)	Total non-linear distance (nm)
Stainless steel	158 ± 20	(-) 35 ± 4	190 ± 20
Glass	180 ± 40	(-) 26 ± 4	210 ± 40
Cellulose	600 ± 80	(-) 71 ± 9	670 ± 90

The errors represent the standard error of the mean from two independent biofilms (each tested at 6 different positions). A negative value of contact phase is a length of probe which is in contact with a polymer on biofilm surface before reaching the constant compliance region

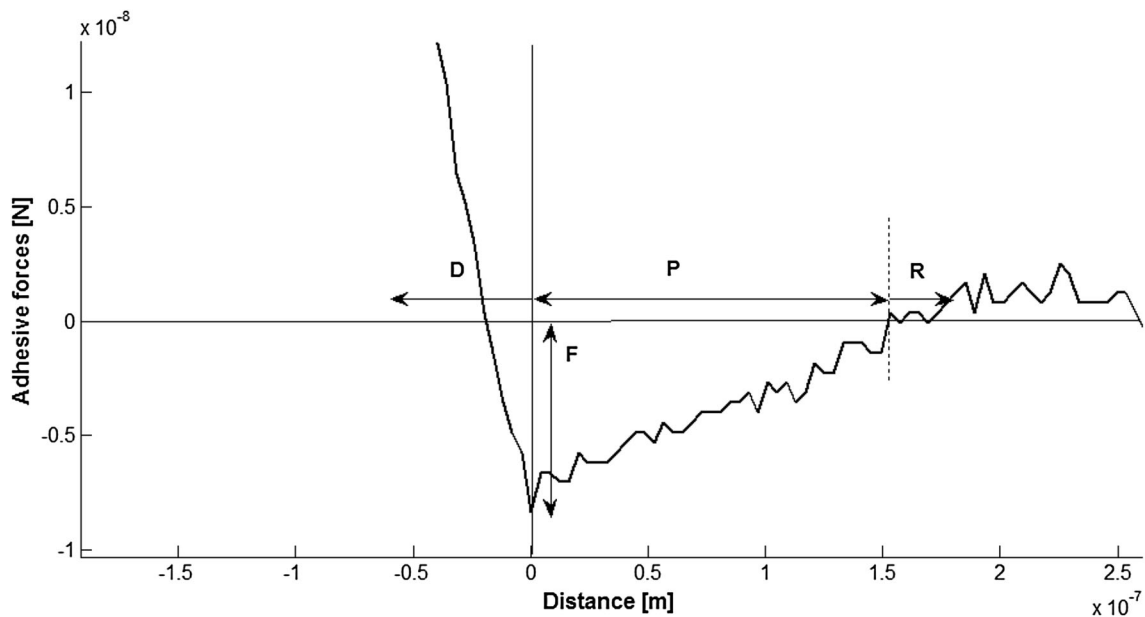


Fig. 4 A representative retraction curve for stainless steel colloidal probe from *P. fluorescens* biofilm at zero contact time. *Region D* the constant compliance region during retraction; *Region P* the maximum pull-off distance; *Region R* a region

where there is no longer interaction between the colloidal probe and the biofilm surface; and *F* the maximum probe-biofilm adhesive force

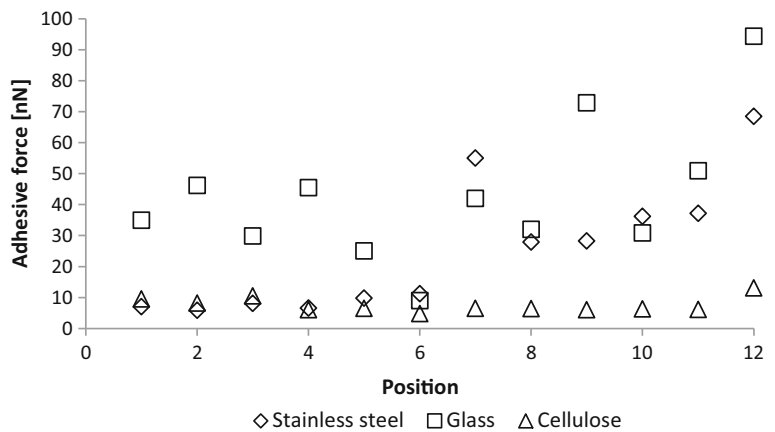
observations and that the theory must be augmented with forces such as steric repulsion and hydrophobic interactions to adequately predict cell adhesion (van Oss 2003).

Whilst a probe was in contact with the biofilm, EPS might have adhered to the probe, leading to the behaviour seen in Fig. 4. There are multiple peaks in the force-distance curve possibly caused by successive breakage of polymer chains attached to the probe. The stainless steel exhibited a pull-off distance of 153 nm, which is defined as a distance between the maximum adhesive force presented in

the retraction curve and a point where the probe is no longer in contact with the biofilm. The area between the base line and the curve can be used to calculate the adhesive energy, which may be important to determine the removal of biofilm by mechanical forces, e.g. fluid flow.

The adhesive forces calculated from the retraction data varied from position to position (Fig. 5). These variations might be due to the heterogeneous nature of biofilms (Fig. 2). However, on average there was significantly greater adhesion of glass and stainless steel to the biofilm than cellulose, which might also

Fig. 5 Distribution of adhesive forces for stainless steel (*open diamond*), glass (*open square*) and cellulose (*open triangle*) probes over 6 positions on 2 independent biofilm samples at zero contact time. The adhesive forces were determined using Hooke's law, the maximum vertical deflection of the cantilever during retraction, and the calibrated cantilever spring constant



be due to the hydrophilic nature of the latter. The stainless steel and glass (or silica) values are higher than found in other studies (Sheng et al. 2007; Yuan and Pehkonen 2009; Abu-Lail et al. 2007) but the adhesive forces will depend on the instrumentation, experimental conditions and strain of *Pseudomonas* so the method was a useful way to compare these materials.

The difference in adhesion between the 3 types of colloidal probe and the biofilm shown in this study implies that different amounts of energy is required to remove the biofilm from the surfaces made of these materials. In industry, there is a standard procedure called “clean-in-place” to remove fouling deposits including biofilm from surfaces. By understanding the adhesion of a given fouling deposit on surface, it should be possible to clean the surface with minimum amounts of water, chemicals and heat.

Conclusions

Interactions between three different material probes and *P. fluorescens* biofilms showed that the probes experienced repulsive forces for more than 100 nm prior to contact. This indicates the involvement of steric repulsion and hydrophobic interactions probably due to EPS in the biofilms. During retraction, glass gave the greatest adhesive force. The method used here allows comparisons between surfaces to which biofilms might adhere, and can be extended to any material for which a colloidal probe can be prepared. Moreover, the results obtained may help to remove the biofilm from these surfaces more effectively, which

can find applications in cleaning of water systems including industrial fermenters, and textile fabrics.

Acknowledgments The authors would like to thank Malaysia of Education Malaysia (MOE), Universiti Teknologi Malaysia, Fundamental Research Grant Scheme (R.J130000.7845.4F428) and Unilever R&D for their financial support. The atomic force microscope used in this research was obtained through Birmingham Science City: Innovative Uses for Advanced Materials in the Modern World (West Midlands Centre for Advanced Materials Project 2), with support from Advantage West Midlands (AWM) and part funded by the European Regional Development Fund (ERDF).

References

- Abu-Lail LI, Liu Y, Atabek A, Camesano TA (2007) Quantifying the adhesion and interaction forces between *Pseudomonas aeruginosa* and natural organic matter. *Environ Sci Eng* 41:8031–8037
- Bowen J, Cheneler D, Walliman D, Arkless SG, Zhang Z, Ward MCL, Adams MJ (2010) On the calibration of rectangular atomic force microscope cantilevers modified by particle attachment and lamination. *Meas Sci Technol* 21:1–9
- Butt HJ (1994) A technique for measuring the force between a colloidal particle in water and a bubble. *J Colloid Interface Sci* 166:109–117
- Daims H, Lückner S, Wagner M (2006) Daime, a novel image analysis program for microbial ecology and biofilm research. *Environ Microbiol* 8:200–213
- Dorobantu LS, Goss GG, Burrell RE (2012) Atomic force microscopy: a nanoscopic view of microbial cell surfaces. *Micron* 43:1312–1322
- Jasevicius R, Baronas R, Kruggel-Emden H (2015) Numerical modelling of the normal adhesive elastic-plastic interaction of a bacterium. *Adv Powder Technol* 26:742–752
- Kang S, Elimelech M (2009) Bioinspired single bacterial cell force spectroscopy. *Langmuir* 25:9656–9659
- Karlsson JO, Gatenholm P (1999) Cellulose fibre-supported pH-sensitive hydrogels. *Polymer* 40:379–387

- Li X, Logan BE (2004) Analysis of bacterial adhesion using a gradient force analysis method and colloid probe atomic force microscopy. *Langmuir* 20:8817–8822
- Liu Y, Yang SF, Li Y et al (2004) The influence of cell and substratum surface hydrophobicities on microbial attachment. *J Biotechnol* 110:251–256
- Puricelli L, Galluzzi M, Schulte C et al (2015) Nanomechanical and topographical imaging of living cells by atomic force microscopy with colloidal probes. *Rev Sci Instrum*, vol 86. Article Number 033705
- Sheng X, Ting YP, Pehkonen SO (2007) Force measurements of bacterial adhesion on metals using a cell probe atomic force microscope. *J Colloid Interface Sci* 310:661–669
- Shephard JJ, Savory DM, Bremer PJ et al (2010) Salt modulates bacterial hydrophobicity and charge properties influencing adhesion of *Pseudomonas aeruginosa* (PA01) in aqueous suspensions. *Langmuir* 26:8659–8665
- van Oss CJ (2003) Long-range and short-range mechanisms of hydrophobic attraction and hydrophilic repulsion in specific and aspecific interactions. *J Mol Recognit* 16:177–190
- van Oss CJ, Chaudhury MK, Good RJ (1988) Interfacial Lifshitz-van der Waals and polar interactions in macroscopic systems. *Chem Rev* 88:927–941
- Yuan SJ, Pehkonen SO (2009) AFM study of microbial colonization and its deleterious effect on 304 stainless steel by *Pseudomonas* NCIMB 2021 and *Desulfovibrio desulfuricans* in simulated seawater. *Corros Sci* 51:1372–1385